NUMERICAL STUDY OF MORPHOLOGICAL CHANGES BY FAR-FIELD TSUNAMI IMPACTS

Sangyoung Son[*], Patrick Lynett[†]

In this study, we present an integrated numerical model for sedimentation by long waves and also investigate morphological changes by far-field tsunami impacts. A set of models, each of which is responsible for hydrodynamics, sediment transport and morphological evolutions, are introduced with a basic concept of morphodynamic physics and are fully connected through two-way approach. Finite volume scheme, which turns out to be stable and suitable for long-term(more than 10 hours) tsunami simulations is used in the numerical discretization. An accuracy and applicability of developed model is evaluated through numerical tests covering one-dimensional or two-dimensional sedimentation problems in the shallow region. Then, we applied developed model to a field-scale tsunami, which had caused a significant bathymetric changes in harbors.

INTRODUCTION

Either on a short-term or on a long-term basis, a coastline defined as the boundary between wet and dry area on the beach evolves in time in response to many physical processes. Our knowledge on the beach evolution process is yet much limited, since it is a complex, systematic process such that all of their surrounding physics as hydrodynamics, morphodynamics, meteorology, geology and even ecology are closely correlated and interact together. Admitting that nearshore hydrodynamics tend to be much chaotic and unpredictable due to the existence of various types of turbulence sources(e.g., wave-breaking), relatively great uncertainty still remains in sediment process(Elfrink and Baldock (2002)). Therefore, over the past decades beach erosion and accretion induced by nearshore currents become of great interest to coastal and ocean engineers because undesirable morphologic changes may occur and result in practical and environmental problem. To improve the capability of predicting coastal sedimentation, a number of researches have been performed through either numerical modeling or experiment observations so far. In this study, we developed an numerical model for sedimentation by long waves. The model is composed of a set of sub-models, each of which is responsible for hydrodynamics, sediment transport and morphological evolutions. An accuracy and applicability of developed model has been evaluated through numerical tests covering one-dimensional or two-dimensional sedimentation problems in the shallow region. Firstly, one-dimensional dam-break flow over the movable bed is simulated by the model and compared with the laboratory data by Fraccarollo and Capart (2002). Secondly, Kobayashi and Lawrence (2004)'s laboratory experiments in a wave flume (L30m, W2.4m and H1.5m) to study beach profile changes under breaking solitary waves is recreated through the present model for the validation under the wave-breaking situation(i.e., turbulence-governing flows). Thirdly, the model is tested through the partially breached dam-break flow case, which had been conducted experimentally in Xiao et al. (2010). Lastly, Goutiere et al. (2012)'s experiment for dam-break flows over movable bed with a sudden enlargement is challenged for the model verification .Throughout these typical sedimentation cases, calculated values agree well with the experimental records when a reasonable parameter is chosen for an empirical formula. Oeanwide, real-scale simulation on 2011 Tohoku-oki tsunami, one of the most destructive tsunamis in history is finally attempted with a focus on the localized effects of tsunami waves on sedimentation at the Santa Cruz Harbor, CA(USA). It has already been reported through observations that tsunami waves had significantly affected morphological features within the harbor(Wilson et al. (2012))). A multi-grids and multi-physics tsunami model is also used for the better reproduction of current fields by tsunami waves in the nearshore(Son et al. (2011), Lynett et al. (2012)). Consistently with the observation that strong currents were induced by tsunami waves in the harbor, large velocity fields have been successfully generated through the model, resulting severe sedimentation processes of scouring and deposition. Good agreements in depth changes and area coverages for scouring and deposition are shown between modeled and observed records.

THEORETICAL APPROACH

In the modeling effort, we coupled separate sub-models as will be explained bellows to appropriately represent a complete modeling system of sediment process. The integrated model has three main com-

[*]Department of Civil and Environmental Engineering, University of Ulsan, South Korea
[†]Department of Civil and Environmental Engineering, University of Southern California, US

ponents; hydrodynamics system, sediment transport system, morphodynamic evolution system. Outlined belows are the model equations along with complete closures used in the models.

Hydrodynamic System

A weakly dispersive and rotational Boussinesq-type modeling approach is used for the hydrodynamic system in this study. A Boussinesq model is a depth-integrated, phase-resolving equations for mass and momentum conservation in the shallow water regime and widely used for nearshore hydrodynamic modeling. Recently, a number of nontraditional Boussinesq approaches have been developed, with the goal of including horizontal vorticity explicitly in the flow field. Kim et al.(2009) has modified equations for rotational fluid flows through the inclusion of bottom-induced turbulence effects as higher-order terms balancing with dispersive effects. Throughout various types of demonstrations, it is shown that the model can be used for more accurate prediction of nearshore modeling inherently involving complex surf and swash hydrodynamics (e.g., wave breaking, undular bores, run-up and run-down). This promising advance of taking into account of bottom-induced rotationality into the model, in the respect of sediment modeling, allows more reliable reconstruction of velocity profile in the nearshore. Making use of rotational Boussinesq equations, therefore, a precise estimation of bed shear stress required for sediment transport calculations is achieved.

Mass conservation and momentum equations are given as,

$$\frac{\partial H}{\partial t} + \nabla \cdot (H\boldsymbol{U}_\alpha) + (M + M^v) = \frac{E - D}{1 - p} \tag{1}$$

$$\frac{\partial HU}{\partial t} + \frac{\partial HU^2}{\partial x} + \frac{\partial HUV}{\partial y} + gH\frac{\partial \zeta}{\partial x} + HM_m^x + U(M + M^v) + B_x = -\frac{(E - D)U}{1 - p} \tag{2}$$

$$\frac{\partial HV}{\partial t} + \frac{\partial HUV}{\partial x} + \frac{\partial HV^2}{\partial y} + gH\frac{\partial \zeta}{\partial y} + HM_m^y + V(M + M^v) + B_y = -\frac{(E - D)V}{1 - p} \tag{3}$$

where $H = \zeta + h$ is total water depth, ζ is surface elevation, h is water depth, and U, V is x and y component of velocity at $-0.531h$. And M, M^v represent second-order correction terms by frequency dispersion and bottom-induced turbulence effects in the mass continuity. Similarly, M_m^x, M_m^y denote a higher-order term including frequency dispersion and bottom-induced turbulence effects, respectively in x and y direction momentum equations. Turbulent eddy viscosity is also included in these terms as v_t^h and v_t^y, which denote decomposed horizontal and vertical components, respectively and τ_i^b is the shear stress on bed. Final term on the left hand side of both momentum equations, B_x and B_y add the effect of turbulent mixing and dissipation related to turbulent backscattering and wave-breaking. Full descriptions for higher-order terms can be found in references such as Son et al. (2011), while some open expressions will be 'closed' by closure models given in later section.

It is also noted that some source terms are added here to 'fixed-bed' Boussinesq model on the right hand side of equation 1, among which e and d are sediment erosion and deposition fluxes respectively, and p is bed porosity(Cao et al. (2004), Xiao et al. (2010)). In the equation 2, a conservative form of momentum equation, a source term on the right hand side is originated from the mass-sediment conservation equation 1. Erosion and deposition fluxes included will be modeled through the sediment transport model as we will see.

Sediment Transport System

Suspended sediments supplied from bottom boundary layer are transported due to the flow motion, until settling down by the gravitational force. Within the long wave assumption, depth-averaged transport model can be utilized to calculate sediment distribution by the flow(e.g., Kobayashi and Johnson (2001), Shimozono et al. (2007)). A depth-integrated sediment transport equation adopted in this study is expressed as, (Cao et al. (2004))

$$\frac{\partial H\overline{c}}{\partial t} + \frac{\partial H\overline{c}U}{\partial x} + \frac{\partial H\overline{c}V}{\partial y} = \frac{\partial}{\partial x}\left(K_h H\frac{\partial \overline{c}}{\partial x}\right) + \frac{\partial}{\partial y}\left(K_h H\frac{\partial \overline{c}}{\partial y}\right) + e - d \tag{4}$$

where $\bar{c}$ is the depth-averaged sediment concentration and K_h is the sediment diffusion coefficient in horizontal plane, assumed to be the same as the flow eddy viscosity (see Rakha et al. (1997)). Sediments entrained by the flow field are governed by transport model above. This model is of typical for the scalar transport, but has additional source or sink terms on the right hand side, which explain the production and annihilation of sediments through erosion and deposition processes, respectively. In this study erosion and deposition fluxes are calculated by empirical formulas.

Morphodynamic Evolution System
We calculated straightforwardly bathymetric changes by sediment fluxes by the equation below. It explains updating process of bathymetry in the Boussinesq and sediment transport models.

$$\frac{\partial h}{\partial t} = \frac{e - d}{1 - p} \tag{5}$$

Closures

Bed Friction For turbulent, shallow flows, shear stress at the bottom boundary is conventionally estimated by quadratic equation,

$$\tau_i^b = C_f \rho U |U| \tag{6}$$

where the friction coefficient, C_f can be approximated by Manning's formula as,

$$C_f = \frac{gm^2}{h^{1/3}} \tag{7}$$

where m is Manning's roughness coefficient.

Bottom-Induced Turbulent Eddy-Viscosity Model In the situation where the bottom friction is in effect to flow fields and generates small to large scale coherent structures, eddies greater than grid size are directly computed through the simulation while ones smaller than grid size(so-called sub-grid scale eddies) are required to be modeled using an appropriate turbulent model. For the horizontal eddy viscosity, Smagorinsky's turbulent eddy viscosity model is utilized as,

$$\nu_t^h = (C_s \Delta x_i)^2 \sqrt{2 \mathcal{S}_{ij} \mathcal{S}_{ij}} \tag{8}$$

in which C_s is a constant, Δx_i is a grid size and $\mathcal{S}_{ij}$ is a strain rate.

Elder's model, on the other hand is adopted for the vertical eddy viscosity as,

$$\nu_t^y = C_h H U^b \tag{9}$$

in which $C_h = \kappa/6$ is used following Elder (1959) and von Karman's constant, κ is set to 0.4 in this study. And U^b refers to a frictional velocity.

Turbulence Back-Scatter Model Turbulence energy transfer from smaller scale than grid size to large scale is known to be particularly significant in boundary layer. To appropriately account for this effect(a.k.a turbulence back-scattering) in the 2HD model, we adopted a stochastic backscatter model(Hinterberger et al. (2007)) which adds some forcing term in the momentum equation.

Eddy-Viscosity Based Wave-Breaking Model It turns out that energetic and chaotic turbulence process occurs during the wave-breaking and is often calculated through eddy-viscosity model. This study utilized an additional term in the momentum equation to take account for the entire procedure of energy dissipation by wave breaking. Full description on the eddy-viscosity based wave-breaking model can be found in Kennedy et al. (2000)).

Erosion and Deposition Flux Sediment exchanges between sediment boundary layer and flow fields are estimated through erosion and deposition fluxes. Therefore, an erosion flux in conjunction with a deposition flux is important part of the coastal sediment modeling. A great number of and various types of formulas have been developed for erosion and deposition estimates under either steady or unsteady flows and are

mostly founded on experimental data. In the present study, an empirical formula proposed by Cao et al. (2004) is adopted.

The erosion flux, e can be obtained by

$$e = \begin{cases} \varphi\,(\theta - \theta_c)\,|U|H^{-1}(D_{50})^{-0.2} & \text{if} \quad \theta \geq \theta_c \\ \\ 0 & \text{else} \end{cases} \tag{10}$$

in which φ is empirical parameter, θ is Shield's parameter, θ_c is critical Shield's parameter, D_{50} is median grain diameter of sediment.

Here Shield's parameter, θ is defined as

$$\theta = \frac{\left(u^b\right)^2}{\left(\rho_s/\rho_w - 1\right)gD_{50}} \tag{11}$$

where ρ_s and ρ_w mean density of sediment and fluid, respectively.

The deposition flux, d can be modeled by the following formula.

$$d = \alpha\bar{c}w_0 \tag{12}$$

where $\alpha = \min\left[2, (1 - p)/\bar{c}\right]$, w_0 is fall velocity defined as,

$$w_0 = \frac{4gD_{50}}{3 \times 0.2^{(\rho_s/\rho_w - 1)}} \tag{13}$$

NUMERICAL SCHEME

In order to manipulate differential equations introduced into discretized ones, we adopted finite volume scheme which turns to be very stable and accurate for long-term simulations. Entire descriptions about finite volume scheme application can be found in references such as Son et al. (2011).

MODEL VALIDATION AND CALIBRATION

To validate the developed model, three typical tests have been attempted. First, one-dimensional dam-break flow over a movable bed is simulated by the model and compared with the laboratory data by Fraccarollo and Capart (2002). The experiment was performed in a channel with 2.5-m length, 0.1-m width and 0.25-m depth, which had 0.1 m initial water depth upstream while a dry condition was initially retained downstream. PVC particles of 3.5-mm diameter with 1,540-kg/m^3 density were used for the movable bed materials. In the numerical simulation, the grid size (dx) is 0.005 m and time step (dt) is dynamically determined by a Courant number of 0.1. The sediment porosity (p) and settling velocity (w_0) are set to 0.3 and 0.18 m/s, respectively, based on Wu and Wang (2008). Manning's coefficient (n) is 0.025, and the empirical coefficient in the erosion flux equation is 0.003. Simulated results compared with measured data are shown in figure 1. Generally good agreement between calculation and measurement is found, while some discrepancies exist in surface elevations near the leading front and hydraulic jump locations.

Recently, Kobayashi and Lawrence (2004) carried out laboratory experiments in a wave flume (length 30 m, width 2.4 m, and height 1.5 m) to study beach profile changes under breaking solitary waves, as shown in figure 2. A solitary wave of 0.216-m height was generated by wave paddle and propagated to the sloping beach composed of sand grains. The water depth beyond the base of the beach was 0.8 m. The beach has initial slope of 1:12 that is expected to be changed by the breaking solitary waves. The solitary wave was repeated eight times to consider the effects by multiple wave attacks. Bottom profiles after four and eight waves, as well as surface elevations at eight locations (G1 to G8) across the beach after four waves, were measured. The median grain diameter (d_{50}), fall velocity (w_0), specific gravity, and porosity (p) are 0.18 mm, 2.0 cm/s, 2.6, and 0.4, respectively.

t=0.505sec

Calculated FSE
○ Measured FSE
Calculated Bed Profile
□ Measured Bed Profile

t=0.757sec

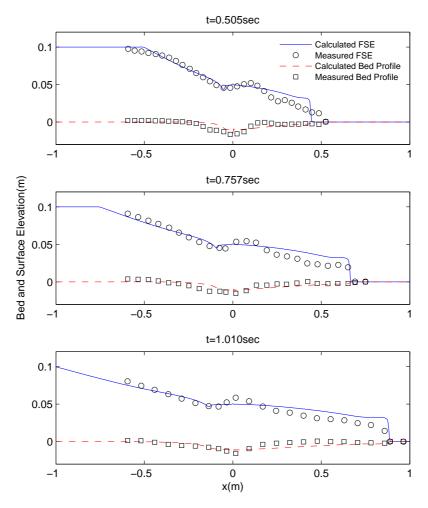Bed and Surface Elevation(m)

t=1.010sec

x(m)

Figure 1: Graphs comparing measured and simulated dam-break flows over a movable bed at different elapse time after dam break. x=0: position of dam. Elevation = 0: initial bed surface elevation
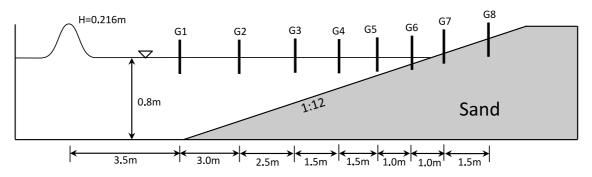
H=0.216m

G1   G2   G3   G4   G5   G6   G7   G8

0.8m

1:12   Sand

3.5m   3.0m   2.5m   1.5m   1.5m   1.0m   1.0m   1.5m

Figure 2: Diagrammatic cross section showing experimental setup for breaking solitary waves on a sloping sand beach
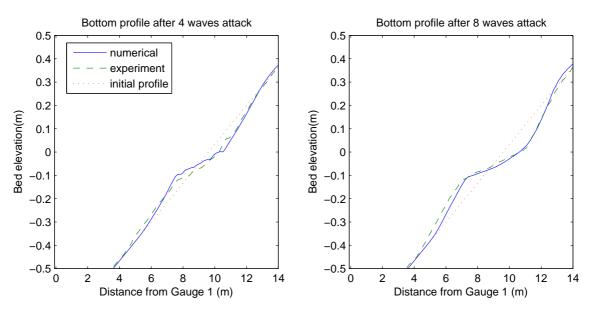
Figure 3: Graphs comparing measured and calculated beach profiles for Kobyashi test

To evaluate the accuracy and performance of the model, their experiment was recreated through numerical modeling using the same conditions as in the experimental setup. The simulation was performed using a uniform grid size of 0.1 m and varying time step with a Courant number of 0.4. For Manning's coefficient (n) and empirical parameter (φ), 0.025 and 7.5×10^{-6} are used, respectively. Additionally, to account for turbulent mixing and dissipation by wave breaking, the eddy-viscosity model proposed by Kennedy et al. (2000) is adopted in the test. Calculated beach profiles compared with the measured data are shown in figure 3. Good agreement is found in both results after four and eight waves. Significant erosion at the foreshore is observed in both measured and computed results, which may be explained by the strong backwash current caused when the solitary wave rushes back down. The entrained sediments are deposited on the seaward side.

Finally, the case of flow in a partially breached dam-break was used to test the present model. This test was conducted experimentally in Xiao et al. (2010). Figure 4 depicts the experimental setup of the test, in which the middle of the channel has a moveable bed section composed of coal ash. The median diameter (d_{50}) of the coal ash was 0.135 mm and the density was 2,248 kg/m^3. Initial water depths were 0.4 m and 0.12 m for upstream and downstream, respectively. Strong jet-like flow through the 0.2-m-wide gap caused significant erosion, and cross-sectional profiles of the bottom were measured at cs1 (x = 2.5 m) and cs2 (x = 3.5 m) after 20 seconds.

The identical situation to this experimental test has been reproduced numerically with a grid resolution of 0.025 m. As in previous tests, our time step varies and is based on a Courant number of 0.3. Following Xiao et al. (2010), Manning's coefficient (n) is set to 0.015 while the empirical parameter is tuned to 5.0×10^{-5}. Fall velocity can be approximated by an empirical formula (Ponce, 1989) because it is not given explicitly in the experimental description. Figure 5 compares the bottom profiles in the simulated and measured data. Reasonable agreement is seen at both profiles cs1 and cs2, but the simulation overestimates the peak erosion depth at cs1. As pointed out by Hinterberger et al. (2007), in depth-averaged 2D modeling, turbulence backscattering needs to be considered when strong horizontal shear exists (as near the breached gap in this test). Through it, turbulence energy transfer from unresolved subdepth scale to the resolved 2D flows can be explained. Figure 6 shows the same results as in figure 5 but with the backscatter model used. Prediction of maximum erosion depth at cs1 is much improved by including backscatter model.

MODEL APPLICATION TO SANTA CRUZ HARBOR, CALIFORNIA

Some recent observations have shown that far-field tsunami events can lead to severe changes in bottom morphology, especially in the nearshore area (Lacy et al. (2012), Wilson et al. (2012)). Because relatively
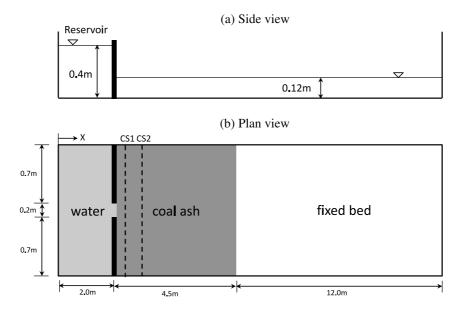
(a) Side view

Reservoir

0.4m

0.12m

(b) Plan view

X

CS1 CS2

0.7m

0.2m

water

coal ash

fixed bed

0.7m

2.0m

4.5m

12.0m

Figure 4: Experimental setup of a dam-break flow through a partial breach over moveable bed

Sectional Bottom Profile at X=2.5m

Bed elevation(m)

distance from side wall(m)

Num
Exp

Sectional Bottom Profile at X=3.5m

Bed elevation(m)

distance from side wall(m)

Figure 5: Measured and calculated bottom profiles of a dam-break flow through a partial breach over moveable bed
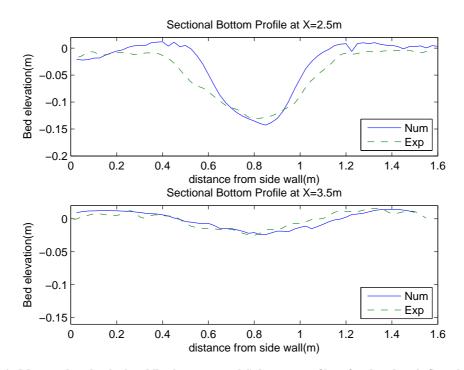
Figure 6: Measured and calculated(Backscatter model) bottom profiles of a dam-break flow through a partial breach over moveable bed

small-amplitude tsunami waves (< 1–2 m) can create strong current fields near harbor basins (see, for example, Son et al. (2011), Lynett et al. (2012)), tsunamis have great potential to mobilize bed sediments. Needless to say, therefore, it is important to estimate tsunami currents accurately in the nearshore area in evaluating morphological changes near the shoreline. Traditional approaches to estimate sediment transport by tsunami waves are based on the shallow-water equation model. As a practical application of the present model to the coastal region, the 2011 Japan tsunami event is considered For precise estimations of current fields from far-field tsunami waves in the nearshore area, a multigrid and multiphysics model developed by Son et al. (2011) was applied to 2011 Japan event. A total of five nested layers were employed, with different levels of resolution. The final layer has the smallest domain focusing only on the Santa Cruz Harbor area, with relatively fine grid size (10 m), and is solved by Boussinesq equations to account for higher order effects by dispersive and turbulent processes. On the other hand, the rest of the layers, which generally cover a larger domain with deeper ocean rather than the shallow coastal region, are solved by shallow-water equations. The parametric values used in the sediment model are the median sediment diameter d_{50} = 0.15mm, Manning's coefficient (n) = 0.025, and the empirical parameter(φ) = 5.0×10^{-5}, which is an acceptable value for coastal sedimentation. The Courant number of the Boussinesq model is set to 0.4. The simulation was performed for 14 hours of tsunami waves at the harbor to allow enough duration for the erosion and sedimentation processes. Resultant bathymetric change at the harbor entrance is shown in figure 7, compared with observed data. The overall pattern of sedimentation and erosion is quite well recreated by the numerical model.
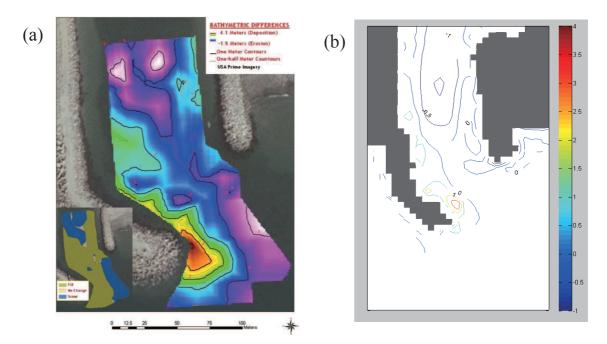
Figure 7: Changes in bottom bathymetry from tsunami-induced currents in Santa Cruz Harbor, California. Left:observed changes in the 2011 Japan tsunami event, excerpted from Wilson et al. (2012). Right:computed bathymetric changes from the simulation. Color scale in meters (positive = deposition; negative = erosion).

CONCLUSION

In this study, we develop numerical model for bathymetric changes by tsunami waves in the nearshore area. Three sub-models are combined to yield a system of sediment modeling. For the better representation of nearshore hydrodynamics in the model, we adopt Boussinesq model which is superior to the shallow water equation model in that it include various, complex nearshore effects; frequency dispersion, bottom shear induced rotationality, bottom-induced turbulence effects. To validate the model, we performed three numerical tests. The result from simulation agree well with experimental data in each case. Finally, we applied developed model to real tsunami event and successfully simulated morphodynamic changes during the tsunami event.

ACKNOWLEDGEMENTS

References

Z. Cao, G. Pender, S. Wallis, and P. Carling. Computational dam-break hydraulics over erodible sediment bed. *Journal Hydraulic Engineering*, 130:689–703, 2004.

J. W. Elder. The dispersion of marked fluid in turbulent shear flow. *Journal of Fluid Mechanics*, 5:544–560, 1959.

B. Elfrink and T. Baldock. Hydrodynamics and sediment transport in the swash zone: a review and perspectivess. *Coastal Engineering*, 45:149–167, 2002.

L. Fraccarollo and H. Capart. Riemann wave description of erosional dam-break flows. *Journal of Fluid Mechanics*, 461:183–228, 2002.

L. Goutiere, S. Soares-Frazao, and Y. Zech. Dam-break flow on mobile bed in abruptly widening channel: experimental data. *Journal of Hydraulic Research*, 49(3):367–371, 2012.

C. Hinterberger, J. Frohlich, and W. Rodi. Three-dimensional and depth averaged large eddy simulations of some shallow water flows. *Journal Hydraulic Engineering*, 133:857–872, 2007.

A. Kennedy, Q. Chen, J. Kirby, and R. Darlymple. Boussinesq modeling of wave transformation, breaking, and runup. i: 1d. *Journal of Waterway, Port, Coastal and Ocean Engineering*, 126:39–47, 2000.

N. Kobayashi and B. Johnson. Sand suspension, storage, advection, and settling in surf and swash zones. *Journal of Geophysical Research*, 106(C5):9363–9376, 2001.

N. Kobayashi and A. Lawrence. Cross-shore sediment transport under breaking solitary waves. *Journal of Geophysical Research*, 109:C03047, 2004.

J. Lacy, D. Rubin, and D. Buscombe. Currents, drag, and sediment transport induced by tsunami. *Journal of Geophysical Research*, 117:C09028, 2012.

P. Lynett, J. Borrero, R. Weiss, S. Son, D. Greer, and W. Renteria. Observations and modeling of tsunami-induced currents in ports and harbors. *Earth and Planetary Science Letter*, 327-328:68–74, 2012.

K. Rakha, R. Deigaard, and I. Broker. A phase-resolving cross shore sediment transport model for beach profile evolution. *Coastal Engineering*, 31:231–261, 1997.

T. Shimozono, S. Sato, and Y. Tajima. Numerical study of tsunami runup over erodible sand dunes. *Proceedings of Coastal Sediments '07*, New Orleans, LA, USA, 2007.

S. Son, P. Lynett, and D.-H. Kim. Nested and multi-physics modeling of tsunami evolution from generation to inundation. *Journal of Geophysical Research*, 38:96–113, 2011.

R. Wilson, C. Davenport, and B. Jaffe. Sediment scour and deposition within harbors in california(usa), caused by the march 11, 2011 tohoku-oki tsunami. *Sedimentary Geology*, 282:228–240, 2012.

W. Wu and S. Wang. One-dimensional explicit finite-volume model for sediment transport with transient flows over movable beds. *Journal of Hydraulic Research*, 46(1):87–98, 2008.

J. Xiao, B. Lin, R. Falconer, and G. Wang. Modelling dam-break flows over mobile beds using a 2d coupled approach. *Advances in Water Resources*, 33:171–183, 2010.